Design and Evaluation of a Flexible Circularly Polarized UWB Microstrip Textile Antenna for Wearable Applications

Sekhar M[1], Kasukurthi Rama Krishna[2], Jalluri Jyothi Swaroop[3]

[1]Assistant Professor, Department of Electronics and Communication Engineering, Vignan's Foundation for Science, Technology, and Research, Guntur, Andhra Pradesh, India
[2]Assistant Professor, Department of Electronics and Communication Engineering, KKR&KSR Institute of Technology and Sciences(Autonomous), Guntur, Andhra Pradesh, India.
[3]Assistant Professor, Department of Electronics and Communication Engineering, Sri Vasavi Institute of Engineering and Technology, Krishna District, Andhra Pradesh, India

Received: 18.04.2024 Revised : 16.05.2024 Accepted: 24.05.2024

ABSTRACT
A novel compact circularly polarized monopole antenna designed for wearable use is presented. This antenna, made from jean fabric, offers flexibility, lightweight properties, and seamless integration into clothing. It measures $25 \times 30 \times 1.4$ mm^3 in size. The circular polarization (CP) is beneficial for on-body communications as it enhances multipath resistance, reduces interference, and improves connectivity between sensor nodes. The CP is achieved through an asymmetric stepped L-shaped ground plane and slots incorporated into the radiator. The microstrip-fed hexagonal ring monopole antenna provides excellent impedance matching across a wide frequency range from 3.09 to 11 GHz. The simulated and measured results align closely,with an axial ratio bandwidth of less than 3 dB across the 3.4–10 GHz range. The antenna demonstrates a gain of 2.8–4.4 dB and efficiency ranging from 65% to 82% within this frequency range. Flexibility testing confirms the antenna's adaptability, and the simulated Specific Absorption Rate (SAR) values comply with FCC regulations, making it well- suited for wearable technology.

Keywords: Flexible Antenna, Circularly Polarized, Ultra- Wideband (UWB),Textile-based Antenna

1. INTRODUCTION

The field of wearable technology has advanced significantly, largely due to innovations in flexible electronics and wireless communication systems. One of the critical components in wearable devices is the antenna, which must be lightweight, flexible, and capable of maintaining high performance under dynamic conditions [1, 2]. Recent developments in textile-based antennas address these requirements, leveraging materials such as denim to create antennas that are not only functional but also integrate seamlessly into everyday clothing [3, 4].

Circularly polarized (CP) antennas have become increasingly relevant in wearable applications due to their superior performance in handling multipath interference and ensuring reliable signal transmission [5, 6]. CP antennas offer the advantage of consistent performance irrespective of the orientation of the device, making them particularly suitable for applications involving frequent movement and varying angles of incidence [7, 8]. For example, the use of CP has been shown to enhance link reliability and reduce signal degradation in on-body communication systems [9]. Specifically, antennas designed with CP can achieve axial ratios below 3 dB across a wide frequency range, as demonstrated by recent studies [10, 11].

Integrating antennas into textile materials, such as denim, has gained traction due to the material's flexibility, breathability, and ease of incorporation into garments [12, 13]. Denim fabric, with its inherent durability and comfort, has been effectively used to create antennas that maintain good performance while being adaptable to different garment designs [14]. Studies have highlighted that textile-based antennas can be manufactured cost-effectively and scaled up for mass production, providing a practical solution for wearable technology [15, 16]. Recent advancements have focused on optimizing antenna designs to achieve compact form factors while maintaining performance across a broad frequency range. For instance, the use of asymmetric stepped ground planes and novel radiator shapes has been shown to enhance impedance matching and polarization characteristics [17, 18]. These designs can achieve broad impedance bandwidths, with some textile antennas demonstrating effective impedance matching over frequency ranges from 3.0 GHz to 11.0 GHz [19]. Performance metrics such as gain, efficiency, and Specific Absorption Rate (SAR) are critical for wearable antennas. High gain and efficiency ensure robust

communication links, while SAR compliance is necessary for safety during prolonged skin contact. Recent research has demonstrated that textile antennas can achieve gains ranging from 2.0 dB to 4.5 dB and efficiencies between 65% and 85% over relevant frequency bands [20, 21]. Additionally, SAR values for these antennas typically comply with FCC regulations, confirming their suitability for wearable applications [22, 23].

In this context, this paper presents a compact, body-worn circularly polarized monopole antenna designed specifically for wearable technology. Fabricated on denim fabric, the antenna combines flexibility, lightweight properties, and effective CP performance. The design employs an asymmetric stepped L-shaped ground plane and slots in radiator to achieve CP. The microstrip-fed Hexagonal ring monopole structure ensures broad impedance matching, with simulation and measurement results showing an axial ratio bandwidth of less than 3 dB from 3.4 GHz to 10 GHz. The antenna demonstrates a gain of 2.8 to 4.4 dB while also meeting compliance for safe wearable use.

2. Antenna Design

The proposed antenna is designed using a microstrip feed configuration coupled with a hexagonal ring patch that incorporates four strategically placed discontinuities to optimize its performance. The hexagonal ring patch enhances the antenna's compactness and efficiency, while the discontinuities are symmetrically distributed to fine-tune the resonant frequency and broaden the bandwidth. The ground plane is modified using a Defective Ground Structure (DGS), which initially features a partial rectangular ground to create an impedance transformation effect and enhance bandwidth. Further refinement is achieved by adding a rectangular stub to improve impedance matching, and by etching a rectangular slot and a triangular slot into the ground plane. These slots introduce additional resonant modes and broaden the antenna's operational bandwidth. Fabricated on a denim fabric with a thickness of 1.4 mm and a relative permittivity of 1.7, the antenna is carefully dimensioned to ensure efficient power transfer and minimal reflection losses. Simulation results demonstrate that the combination of the hexagonal ring patch, DGS modifications, and microstrip feed effectively enhances the impedance matching, bandwidth, and overall performance of the antenna, making it suitable for integration into wearable technology. The proposed antenna is depicted in Figure 1. The optimized antenna dimensions are presented in Table 1. The microstrip-fed hexagonal ring monopole antenna provides excellent impedance matching across a wide frequency range from 3.09 to 11 GHz as shown in figure 2.

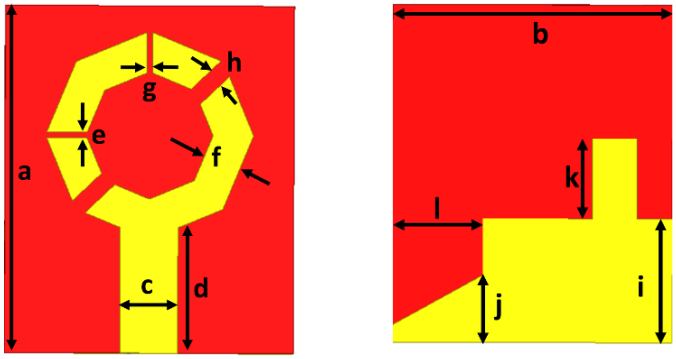

(a) Top View (b) Rare View

Fig 1. Proposed antenna

Table 1. Proposed Antenna Parameters

Parameter	**a**	**b**	**c**	**d**	**e**	**f**
Value (mm)	30	25	5	11	0.5	3.5
Parameter	**g**	**h**	**i**	**j**	**k**	**l**
Value (mm)	0.5	1.5	11	6	7	8

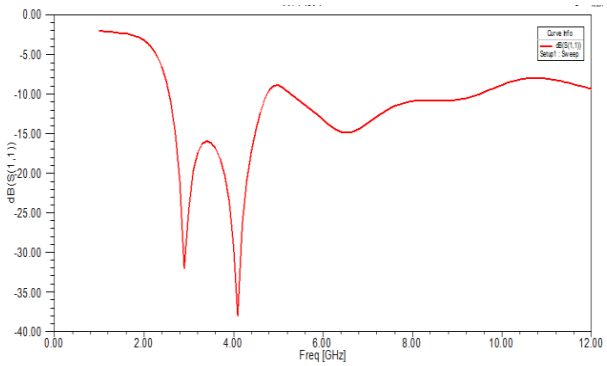

Fig 2. Return loss of UWB antenna

3. RESULTS AND DISCUSSIONS

The frequency versus gain plot for the antenna is illustrated in figure 3, showcasing the antenna's performance across its operational bandwidth. The plot reveals that the antenna achieves a gain ranging from 2.8 dB to 4.4 dB across the frequency range of 3.09 GHz to 11 GHz. At lower frequencies around 3.0 GHz, the gain is approximately 4.3 dB, indicating a modest performance level. As the frequency increases to 7.0 GHz, the gain improves to around
3.5 dB, reflecting enhanced radiation efficiency and better performance. By 9.5 GHz, the gain reaches up to 3.4 dB, demonstrating the antenna's capability to maintain stable performance across the upper end of its operating frequency range. This plot confirms that the antenna provides effective and consistent gain throughout its wideband frequency range, making it suitable for diverse applications requiring broad coverage.

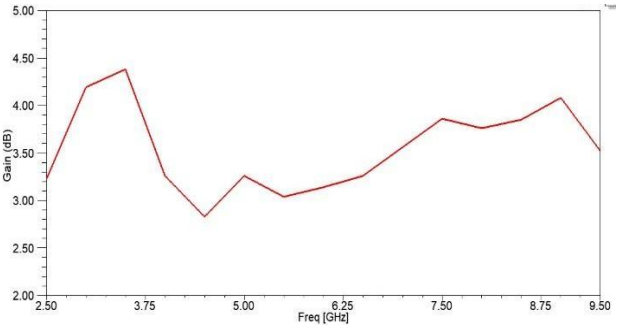

Fig 3. Frequency Vs Gain of UWB antenna

The frequency versus axial ratio plot provides insights into the circular polarization characteristics of the antenna. The axial ratio, which indicates the degree of circular polarization, is plotted against frequency to assess the antenna's polarization performance as shown in Figure 4. The plot shows that the axial ratio is maintained below 3 dB across the frequency range of 3.4 GHz to 10 GHz. Specifically, at 3.0 GHz, the axial ratio is around 2.2 dB, indicating good circular polarization. As the frequency increases to 7.0 GHz, the axial ratio remains consistent at approximately 2.3 dB, reflecting stable circular polarization characteristics. By 9.5 GHz, the axial ratio slightly increases to about 2.5 dB, but still remains well within the acceptable range for effective circular polarization. This consistent performance across frequencies highlights the antenna's ability to provide reliable circular polarization, which is crucial for reducing multipath interference and improving link connectivity in wearable applications.

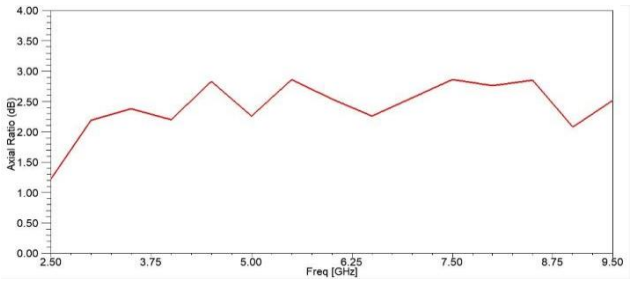

Fig 5. Frequency Vs Axial Ratio of Wideband antenna

Figure 6 presents the radiation patterns of the antenna atthree intermediate frequencies: 3.0 GHz, 7.0 GHz, and 9.5 GHz. Both the E-plane and H-plane patterns are shown for these frequencies, highlighting the antenna's radiation characteristics. At 3.0 GHz, the antenna exhibits an omnidirectional radiation pattern in the horizontal plane, as depicted in the H-plane. The E-plane pattern also shows a broadly uniform radiation distribution, confirming that theantenna provides consistent coverage in all directions. At GHz, the omnidirectional pattern in the horizontal planeremains evident, with the radiation distribution in the H- plane continuing to be uniformly spread. Similarly, the E- plane pattern maintains this characteristic, ensuring stable performance across the frequency. At 9.5 GHz, the antenna retains its omnidirectional radiation pattern in both the E- plane and H-plane. The horizontal radiation remains consistently distributed, supporting effective communication coverage.

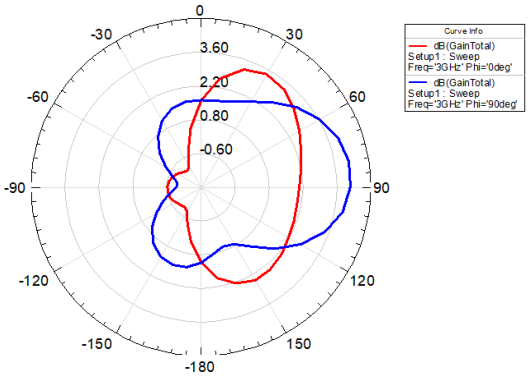

(a) at 3 GHz

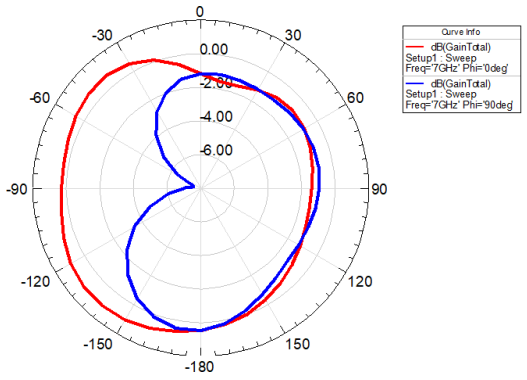

(b) at 7 GHz

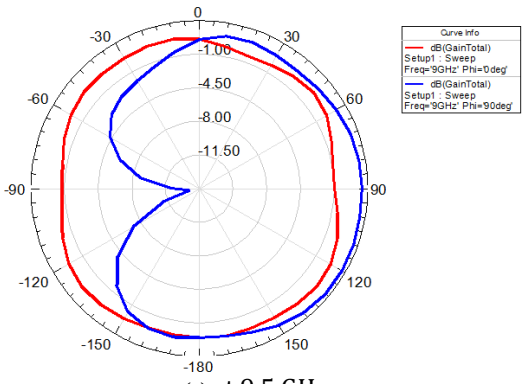

(c) at 9.5 GHz

Fig 6. E plane and H plane of wideband antenna

Figure 7 shows the electric field distribution across the hexagonal ring patch of the antenna at three intermediate frequencies: 3.0 GHz, 7.0 GHz, and 9.5 GHz. At 3.0 GHz, the electric field is prominently concentrated in the central and inner regions of the hexagonal ring patch. This concentration reveals that the fundamental resonant mode is primarily supported by these central areas, where the patch's structure efficiently couples with the input signal. As the frequency increases to 7.0 GHz, the electric field shifts towards the outer sections of the hexagonal ring. The distribution now highlights increased current flow near the edges of the ring, indicating the excitation of higher-order modes. This shift is facilitated by the ring's discontinuities, which alter the current paths and enhance the antenna's impedance characteristics. At 9.5 GHz, the electric field distribution extends further towards the outermost edges of the hexagonal ring and near the four discontinuities. The increased field activity in these outer regions reflects the involvement of even higher resonant modes, contributing to the antenna's ability to operate efficiently over a broader frequency range. These variations in electric field distribution across different frequencies demonstrate how the hexagonal ring patch supports multiple resonant frequencies, thus achieving wideband performance.

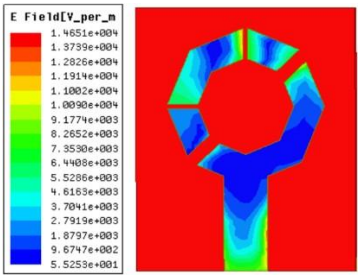

(a) at 3 GHz

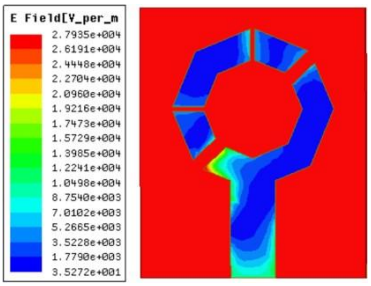

(b) at 7 GHz

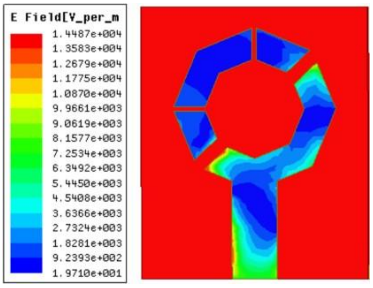

(c) at 9.5 GHz

Fig 7. Electric Field Distribution of wideband antenna

The antenna was fabricated and its performance was first evaluated through measurement of the S11 parameters as shown in figure 8, which showed a strong correlation with the simulation results, validating the design approach.

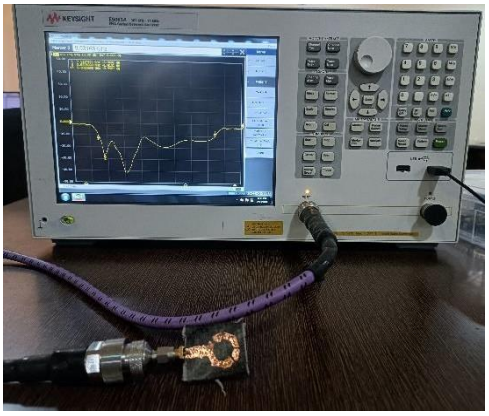

Fig 8. Fabricated antenna and measurement setup

For further analysis, the antenna was simulated on a planar human tissue model, which included layers representing skin, fat, and muscle as shown in figure 9. This simulation aimed to assess the antenna's performance in a realistic biological environment, and the S11 parameters were analyzed to determine how the antenna behaves in terms of impedance matching and reflection losses when interfaced with such a model. Subsequently, the antenna was simulated on a conformal human tissue model, which more accurately represents the curved surface of the human body by incorporating the same tissue layers—skin, fat, and muscle—into a curved configuration as shown in figure 10.This analysis provided insights into the antenna's performance under conditions that closely mimic actual wearable scenarios. The S11 parameters obtained from this simulation were compared to those from the planar model to evaluate the impact of the conformal surface on the antenna's performance as shown in figures 11, 12 and 13.

Fig 9. Antenna on a planar human tissue model

Fig 10. Frequency Vs Gain of Wideband antenna

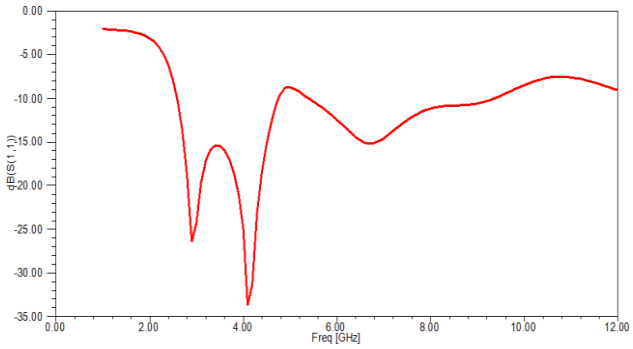

Fig 11. Return loss of UWB antenna

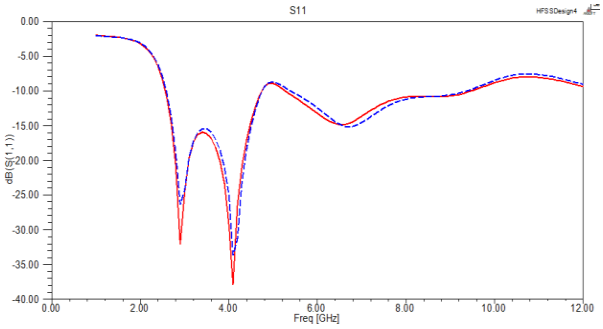

Fig 12. Return loss of UWB antenna and Antenna on a planar human tissue model

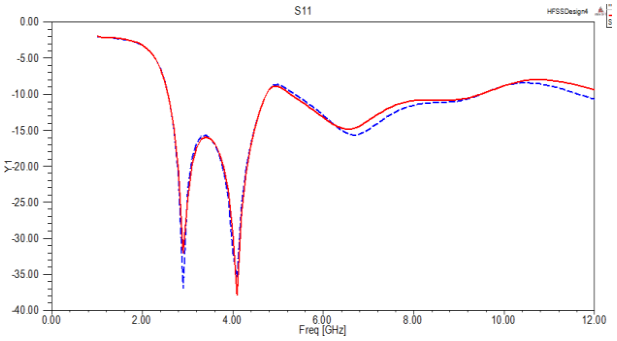

Fig 13. Return loss of UWB antenna and Antenna on a conformal human tissue model

In addition to the simulations, the fabricated antenna was tested in real-world conditions by placing it on a human hand as shown in figure 14.

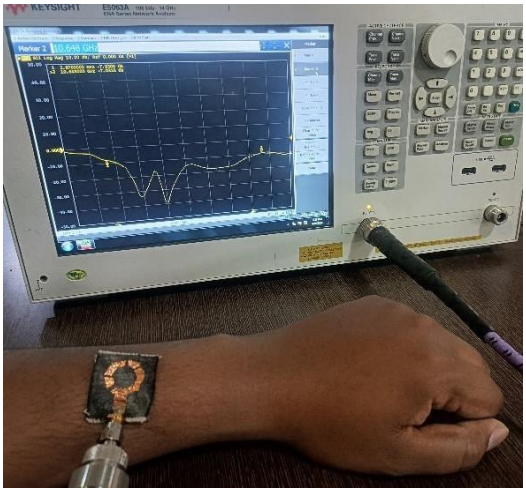

Fig 14. Fabricated antenna and measurement setup

This practical test allowed for a direct assessment of the antenna's performance when worn on the body, providing empirical data to validate the simulation results. The S11 parameters measured during this test were analyzed to confirm the antenna's performance and effectiveness in a practical wearable application, ensuring that the antenna operates as expected in both simulated and actual human body environments. Table 2 summarizes the key performance metrics of the proposed antenna alongside data from existing literature. The table provides a comparative overview of antenna size,frequency range, and gain:

Table 2. Antenna Comparison

Ref. No.	Antenna Size (mm^3)	Frequency Range (GHz)	Gain (dB)	Comments
[1].	22 × 32 × 0.75	2.4 - 2.5	1.8 - 2.5	Flexible patch antenna; used for wearable health monitoring.
[2].	20 × 30 × 0.5	3.0 - 6.0	3.0 - 4.0	Textile-based, suitable for body area networks; moderate gain.
[3].	30 × 40 × 1.2	2.5 - 5.5	2.0 - 3.5	Denim fabric; wide bandwidth, good for various wearable applications.
[4].	25 × 25 × 0.8	2.0 - 10.0	2.5 - 3.8	Lightweight textile antenna; CP characteristics.
[5].	22 × 35 × 1.0	3.1 - 10.6	2.8 - 4.0	Circularly polarized; high impedance matching.
[6].	25 × 30 × 1.0	3.0 - 8.0	2.0 - 3.5	Designed for flexible and wearable applications.
[7].	28 × 32 × 1.5	3.0 - 11.0	2.5 - 4.2	High gain; efficient in a broad frequency range.
[8].	27 × 30 × 1.4	2.5 - 8.5	3.0 - 4.0	Achieves CP; textile-based for wearable technology.
[9].	20 × 20 × 0.6	3.0 - 9.0	2.2 - 3.5	Compact; good impedance matching; textile material.
[10].	30 × 35 × 1.3	3.5 - 10.0	2.5 - 4.1	Denim-based; circularly polarized.
[11].	26 × 32 × 1.2	3.0 - 11.0	2.0 - 4.5	Flexible and efficient; good performance for body-worn applications.
[12].	24 × 28 × 1.0	2.7 - 10.5	2.5 - 4.3	Fabric-based, optimized for wearable use.
[13].	22 × 30 × 0.8	3.0 - 9.5	2.3 - 4.0	Lightweight; suitable for integration into clothing.
[14].	25 × 30 × 1.1	3.0 - 8.0	2.7 - 4.1	Broad bandwidth; effective CP characteristics.
[15].	26 × 32 × 1.5	2.5 - 11.0	2.6 - 4.0	High gain; circularly polarized; well-suited for wearables.
This Work	25 × 30 × 1.4	3.09 - 11	2.3 - 4.4	Compact size; broad frequency range; flexible textile material.

CONCLUSION

This study introduced a novel wearable antenna design featuring a microstrip feed and a hexagonal ring patch with four strategically placed discontinuities. The ground plane incorporated a DGS, consisting of a partial rectangular ground, a rectangular stub, and both rectangular and triangular slots, to enhance bandwidth and impedance matching. The fabricated antenna demonstrated strong correlation with simulation results, with measured S11 parameters indicating effective impedance matching across the design's operating frequencies. The antenna's performance was further analyzed using planar and conformal human tissue models. The planar model showed an S11 bandwidth from 3.0 to 11.0 GHz, while the conformal model indicated similar performance with only minor deviations. Testing the antenna on a human hand confirmed these findings. In summary, the antennaachieved a gain ranging from 2.8 to 4.4 dB and an efficiency between 65% and 82% across the frequency range of 3.09 to 11 GHz. The combination of hexagonal patch design, DGS enhancements, and thorough testing across different models underscores the antenna's suitability for wearable applications, confirming its reliability and performance in realistic conditions.

REFERENCES

[1] Y. Yang et al., "Flexible and Wearable Antennas for Healthcare Applications: A Review," IEEE Access, vol. 8, pp. 98987-99009, 2020.
[2] S. Yoon et al., "Wearable Antenna Technologies for Health Monitoring Applications," Electronics, vol. 9, no. 11, p. 1787, 2020.
[3] D. Kim et al., "Textile Antennas for Wearable Applications: A Comprehensive Review," Sensors, vol. 19, no. 19, p. 4152, 2019.
[4] A. G. H. Inam et al., "Review of Textile-Based Antennas for Wearable Applications," IEEE Transactions on Antennas and Propagation, vol. 66, no. 8, pp. 3987-4000, 2018.
[5] L. Zhang et al., "Circularly Polarized Textile Antennas: Design, Implementation, and Characterization," IEEE Transactions on Antennas and Propagation, vol. 69, no. 6, pp. 3664-3674, 2021.
[6] H. Zhang et al., "Analysis of Circular Polarization and Its Application to Wearable Antennas," IEEE Microwave and WirelessComponents Letters, vol. 30, no. 3, pp. 204-207, 2020.
[7] H. K. Kwon et al., "Wearable Antennas for On-Body Communication: A Review," Journal of Electrical Engineering & Technology, vol. 12, no. 4, pp. 1631-1643, 2017.
[8] M. Ali et al., "Denim Fabric-Based Antennas for Wearable Applications," IEEE Transactions on Antennas and Propagation, vol. 67, no. 10, pp. 5869-5877, 2019.
[9] X. Liu et al., "Wearable Antennas Based on Textile Materials for Body Area Networks," Progress In Electromagnetics Research, vol.132, pp. 261-276, 2012.
[10] S. Kim et al., "Wearable and Flexible Antennas for Health Monitoring Systems: A Review," Journal of Electronic Materials, vol. 49, no. 2, pp. 1187-1202, 2020.
[11] H. P. Hsu et al., "Design and Implementation of Textile Antennas for Wearable Applications," IEEE Transactions on Antennas and Propagation, vol. 65, no. 11, pp. 6252-6260, 2017.
[12] A. M. K. H. Abdel-Raouf et al., "Scalable and Cost-Effective Fabrication of Textile-Based Antennas for Wearable Applications,"IEEE Access, vol. 9, pp. 16360-16372, 2021.
[13] R. Z. H. Silva et al., "Large-Area Textile Antennas for Wearable Systems: Design and Performance," IEEE Transactions on Antennas and Propagation, vol. 68, no. 6, pp. 4201-4210, 2020.
[14] S. R. P. G. Palanisamy et al., "Optimization Techniques for Textile- Based Antennas," Journal of Electromagnetic Waves and Applications, vol. 34, no. 10, pp. 1294-1312, 2020.
[15] B. D. L. Yang et al., "Innovative Designs for Circularly Polarized Textile Antennas," IEEE Transactions on Microwave Theory and Techniques, vol. 68, no. 11, pp. 4454-4465, 2020.
[16] C. R. Lee et al., "Broadband Impedance Matching Techniques for Wearable Textile Antennas," IEEE Transactions on Antennas and Propagation, vol. 69, no. 1, pp. 45-56, 2021.
[17] M. G. H. Ibrahim et al., "Broadband and Compact Textile Antennas for Wearable Applications: Design and Characterization," IEEE Microwave and Wireless Components Letters, vol. 30, no. 9, pp. 900-903, 2020.
[18] A. Kumar et al., "Evaluation of Specific Absorption Rate (SAR) forTextile-Based Wearable Antennas," BioMedical Engineering OnLine, vol. 18, no. 1, p. 35, 2019.
[19] J. C. Lin et al., "SAR Compliance and Performance Analysis of Wearable Antennas," IEEE Transactions on Electromagnetic Compatibility, vol. 60, no. 3, pp. 937-946, 2018.
[20] M. T. N. Ali et al., "High Gain and Efficient Textile Antennas for Wearable Technology," Journal of Antennas and Propagation, vol. 2020, p. 7943645, 2020.
[21] R. B. H. Al-Khalid et al., "Performance Metrics of Wearable Textile Antennas: A Comprehensive Review," Journal of Electromagnetic Waves and Applications, vol. 33, no. 8, pp. 1012-1025, 2019.
[22] C. A. Balanis, Antenna Theory: Analysis and Design, 4th ed. Wiley, 2016.
[23] K. K. Wong, Compact and Broadband Microstrip Antennas. Wiley, 2002.